Effect of soil horizon stratigraphy on the microbial ecology of alpine paleosols

Young, J. M., Skvortsov, T., Kelleher, B. P., Mahaney, W. C., Somelar, P., & Allen, C. C. R. (2019). Effect of soil horizon stratigraphy on the microbial ecology of alpine paleosols. *Science of the Total Environment*, *657*, 1183-1193. https://doi.org/10.1016/j.scitotenv.2018.11.442

Published in:
Science of the Total Environment

Document Version:
Peer reviewed version

Effect of soil horizon stratigraphy on the microbial ecology of alpine paleosols

Jonathan M. Young[1]*, Timofey Skvortsov[2], Brian P. Kelleher[3], William C. Mahaney[4], Peeter Somelar[5], Christopher C.R. Allen[1]

[1]School of Biological Sciences, Queen's University Belfast, UK.

[2]School of Pharmacy, Queen's University Belfast, UK.

[3]School of Chemical Sciences, Dublin City University, Ireland.

[4] Quaternary Surveys, 26 Thornhill Ave, Thornhill, Ontario, Canada

[5] Department of Geology, Tartu University, Tartu, Estonia

*Author for correspondence.

1 ABSTRACT

There is remarkable potential for research at the interface between the earth sciences and environmental microbiology that may lead to advances in our understanding of the role of bacterial communities in the surface or subsurface environment of our planet. One mainstay of sedimentary classification is the concept of differential soil and/or paleosol horizons being the result of primarily physical and chemical weathering, with relatively little understanding of how microbial communities between these stratified horizons differ, if at all. In this study we evaluate the differences in microbial community taxonomy and biogeochemical functional potential between stratified soil horizons in an alpine paleosol environment using next-generation sequencing (NGS) shotgun sequencing. Paleosols represent a unique environment to study the effect of differences soil horizon environments on the microbial community due to their relative isolation, and the fact that three distinct stratified soil horizons can be identified within the top 30cm of the soil. This enables us to assess variation in microbial community composition that will be relatively distinct from variation

due to distance alone. We test the hypothesis that variation in soil community composition is linked to variation in the physical and chemical parameters that define stratigraphy. Multivariate statistical analysis of sequencing reads from soil horizons across five sampling sites revealed that 1223 microbial genera vary significantly and consistently in abundance across stratified soil horizons at class level. Specifically Ktedonobacter, Bacilli and Betaproteobacteria responded most strongly to soil depth. Alpha diversity showed a positive correlation with soil depth. Beta diversity, however, did not differ significantly between horizons. Genes involved in carbohydrate and nitrogen metabolism were found to be more abundant in Ah horizon samples. Closer inspection of carbohydrate metabolism genes revealed that genes involved in CO_2 fixation, fermentation and saccharide metabolism decreased in abundance with depth while one-carbon metabolism increased down profile.

2 INTRODUCTION

Soil microbiology is a rapidly growing discipline, driven by the advances in high throughput sequencing and bioinformatic techniques. Microbiological studies on alpine soils to date have focused mainly on alpine forest, meadow and grassland soils (Ding et al., 2015; Yashiro et al., 2016; Zhang et al., 2013), comparatively little work has been carried out on cold, high altitude alpine soils and paleosols above the timberline (termed the alpine zone; Mahaney et al., 2016). Studies which have focused on soils/paleosols within the alpine zone, such as glacier forefields, have utilised techniques such as amplicon sequencing of the 16S rRNA gene, restriction fragment length polymorphism (RFLP) and/or GeoChip microarrays (He et al., 2007) to assess microbial populations (Lazzaro et al., 2015; Zhang et al., 2013). These

techniques are subject to significant limitations and potential biases, that can now be addressed using shotgun sequencing approaches coupled with bioinformatics.

Several studies have shown that the number of high alpine ecosystems may be expanding worldwide, due to an increase in glacier and ice cap thawing rates (King et al., 2011; Byers, 2008; Zemp et al., 2006)), although there is a chance that increased temperature may reverse this trend by expanding forest to higher elevations (Körner and Paulsen 2004). Regardless, concerns are rising regarding the potential implications this may have for global atmospheric carbon levels as soils are a major carbon sink: soil organic matter contains approximately 3 times the size of the atmospheric pool of carbon and 4.5 times that of the biotic pool (Lal, 2004). Much more organic carbon exists in soils than in vegetation and the atmosphere combined, and the global carbon budget can be strongly influenced by changes in soil carbon content (Fierer et al, 2009; Serna-Chavez et al, 2013). Thawing permafrost in soils newly exposed to increased temperature may increase the rate at which soil microbes degrade soil organic carbon thus leading to a net increase in CO_2 emissions (Davidson and Janssens, 2006). Additionally, the rate of methanogenesis could potentially increase, due to an increase in available metabolites for methanogens (such as acetate), generated as by-products from organisms carrying out soil organic carbon degradation, which could lead to a net increase in methane emissions. Though these sediments are not completely anaerobic, soils in general become more anoxic with increasing depth (Yu et al., 2006). Additionally even in well oxygenated soils, methanogenesis can still occur due to the presence of anoxic microenvironments within soil aggregates (Fierer 2017). Without a more thorough understanding of the functional potential of the microbial communities present in these soils we cannot make predictions as to the possible effects of an increase in exposed alpine soils.

The alpine paleosols studied in this report have developed from the weathering of parent material deposited during two periods following the last glaciation: The Bølling – Allerød warming of ~15-12.8 ka and the Younger Dryas (YD) from 12.8-~11.5 ka (Mahaney et al., 2017). Moraines (deposits of glacial debris described here) from both pre-YD and YD time are evident at elevations greater than 2400m above sea level in this region of France/Italy. The paleosols in these deposits are classified as Cryochrepts (i.e. cold-climate pedons) with Ah/Bw/Cox profiles over fresh undifferentiated, unweathered substrates. In geological terms the soils are identified as paleosols, and they possess distinct stratigraphy with 'classically' identified Ah/Bw/Cox soil horizons (Mahaney et al., 2013). The soils in this study are generally acidic with pH ranging from 4.0-6.0 (supplementary data file 1).

How microbial communities vary with respect to these soil horizons still remains an underexplored avenue of research in soil-paleosol microbial ecology. Of very few relevant published studies, those which compare soil-paleosol horizons either employed 16S rRNA gene amplicon sequencing (Baldrian et al., 2012; Mahaney et al. 2016) or focused specifically on certain functional enzymes, such as dehalogenation enzymes (Weigold et al., 2016). No studies have focused on changes in overall microbial community structure in relation to paleosol stratigraphy.

The alpine paleosols studied here present a unique opportunity to address this apparent gap in knowledge due to:

i. The fact that they possess well stratified horizons, being distinguishable horizons in physical terms.

ii. The wealth of geochemical data already available for the region (e.g. Mahaney et al., 2016; Mahaney and Keiser, 2013).

iii. Their isolation from the Anthropocene: as paleosols these soils are relatively undisturbed by human activity until now, allowing us to assess the effect of >10,000 years of isolated soil development. Their evolutionary history initiated in the Late Pleistocene coming up to their present state in the Late Holocene entitles them to the 'paleo' designation.

There are a number of soil classification systems in current use (Eswaran, 2003), these varying by country and utility (e.g. assessing the suitability of the soil for agricultural use, or inferring its geological origin). In this study soils have been classified according to the United States Department of Agriculture (USDA) soil taxonomy system (USDA, 1999). In this system, a distinct soil horizon is classified as a layer of minerals and organic material, which differs from the parent material in mineral, physical, chemical, morphological, and biological features.

In this study, using high throughput shotgun sequencing, we first aimed to test the hypothesis that microbial communities vary significantly and consistently between stratified soil horizons in an alpine paleosol environment, both in terms of their taxonomic profile and functional potential. We then test the hypothesis that variations in the soil microbiome can be linked to variations in the physical and chemical properties of the soil horizons. Finally, we investigated which taxa and functional gene categories showed the strongest changes in abundance *between* soil horizons.

3 Methods

Sites were selected on the basis of air photo interpretation (1:20,000 scale) of deposits. Clasts embedded in major landform surfaces and profiles (Fig. 1) were sampled following

excavation of sections to depths of ~0.8 m. Profiles extend to depths of ~40-50 cm ± 5 cm. Paleosol descriptions follow standard nomenclature (NSSC, 1995) and Birkeland (1999). The 'Cox' horizon designation, originally defined by Birkeland (1999), is applied to strata with detectable levels of secondary Fe hydroxides and oxides, whereas 'Cu' refers to unweathered parent material (Hodgson, 1976). The 'Ah' horizon designation is applied when surface color is stronger than 10YR 3/1, an indication of appreciable organic carbon accumulation (Canada Soil Survey Comm., 1998). Soil colors were assigned using Oyama and Takehara's (1970) soil colour chips. Bulk samples (250-300 g) were collected from paleosol horizons for particle size, clay mineral, geochemical and microbiological analyses.

DNA was extracted from alpine paleosol samples using a PowerSoil DNA extraction kit (Mo Bio). For each DNA extraction 0.25g of sample was used per extraction, extractions were performed in triplicate and pooled. Extractions were performed according to the manufacturer's protocol with the following modifications: samples were homogenised using a FastPrep 120 cell disrupter system (Thermo-Fisher) at 5.5 $m.s^{-1}$ for 2 minutes, rather than a standard bench top vortex. The eluted and pooled DNA was further purified via two rounds of ethanol precipitation; DNA solution was suspended in 3 volumes of ice cold 100% ethanol, 0.1 volumes 5 M sodium acetate solution (pH 5.2) and 2 µL of linearized polyacrylamide (LPA), the solution was then incubated overnight at -20°C and centrifuged at 18000 x g at 4°C for 30 minutes. The supernatant was discarded and the pellet washed in 70% ice cold ethanol and again centrifuged at 18000 x g at 4°C for 5 minutes. Finally, the supernatant was discarded and the pellet allowed to air dry for 15 minutes before resuspension in 50 µL molecular grade H_20. Final DNA concentrations were measured using a Quantus Fluorometer (Promega) in conjunction with the Quantiflour DsDNA dye system

(Promega). Soil physical and chemical variables were measured as previously described (Mahaney et al., 2016)

Sequencing read quality, length and adapter contamination were initially assessed using Fastqc (Andrews, 2010). Adapter trimming was performed using bbduk from the bbtools package (Bushnell, 2015) using the provided library of Illumina adapters. Quality trimming was also performed using bbduk form the bbtools package, reads were trimmed to a minimum quality score of 20 over a sliding window of 10 bases, additionally the flag 'modulo = 5' was used to remove trailing single odd numbered bases (i.e. the 301st base in a 300bp library, or the 101st base in 100bp library), which are common error bases in Illumina datasets. Read merging was performed using bbmerge from the bbtools package. Human DNA contaminants were removed by using removehuman.sh from the bbtools package. Briefly, raw reads are mapped onto a prebuilt index of the human genome which had been masked to hide 1) any low complexity repeat regions and 2) any regions which showed > 85% identity to any sequence in the Silva rRNA database (Quast *et al.*, 2013) over a 70 base-pair window. This method removes potential human DNA contamination while minimising false positive hits to low complexity regions and ribosomal RNA sequences

Assembly benchmarking was performed using three *de-novo* genome assemblers optimized for metagenomic data, Megahit (Li *et al.*, 2016), SPAdes (Bankevich *et al.*, 2012) (with the flag: – meta), and IDBA-UD (Peng *et al.*, 2012), using kmers ranging from 27-127 in steps of 10. Benchmarking was performed against un-normalized raw reads and reads normalized to minimum kmer depth of 3 and maximum kmer depth of 100 for kmers of size 32. Normalization was performed using bbnorm form the bbtools package, with the flags *min=3, max=100, k = 32*. Read recruitment for each assembly was estimated using bbmap

with the flags *k=13 vslow=t*. Annotation of quality trimmed reads was achieved using Kaiju (Menzel *et al.*, 2016). A database of all proteins from all bacteria, archaea, single celled eukaryotes and viruses in the NCBI non-redundant protein database (NCBI Resource Coordinators, 2017) was constructed using the makeDB.sh script supplied with Kaiju. Nucleotide reads were translated into amino acid sequence in all 6 reading frames and taxonomically annotated by alignment against this database using Kaiju, with a maximum of 5 mismatches allowed and a minimum bit score of 60. Reads were projected onto all taxonomic ranks from phylum to species and per-sample abundances were compiled into single data tables for downstream statistical analysis using a custom bash script. Functional annotations were assigned by mapping NCBI accession IDs from the Kaiju analysis onto functional classifications from the SEED subsystems protein hierarchy (Overbeek *et al.*, 2005) at levels 1, 2 and 3 using MEGAN 6 (Huson *et al.*, 2016).

All taxonomic and functional annotations and read counts were concatenated and downstream analysis was performed using R 3.4.1 (R Core Team, 2011). Taxonomic and functional abundances were summed at each taxonomic and functional rank and normalized by dividing counts for each sample by the total number of reads that were annotated for that sample using the *aggregate* function. Prior to statistical analysis, taxonomic and functional abundance values were Hellinger transformed as described in Legendre and Gallagher, (2001) using the function *decostand* from the package vegan (Oksanen *et al.*, 2016). Soil abiotic variables were log transformed and standardized such that each variable had a mean of zero and standard deviation of 1 across all samples.

Euclidean distance dissimilarity matrices were produced for normalized abundance and abiotic variable tables using the *vegdist* function from vegan. Principal component analysis was performed using the *capscale* function in vegan, samples were plotted in two dimensional space using their first two principal components, plots were produced for taxonomic abundances at the class and genus levels, for functional abundances, and for soil abioitic variables. For taxonomic annotation tables, genus-level richness and Shannon-Weaver diversity indices were computed using the diversity function from the package vegan. Beta diversity for each soil horizon was inferred for all taxonomic and functional ranks as the distance to the group centroid in Euclidean space using the *betadisper* function from the package vegan. Analysis of variance (ANOVA) tests were performed to test for significant differences between group beta dispersions using the function *anova*. Analysis of similarities (ANOSIM) (Clarke, 1993) was performed on all samples grouped by biome type, sample site (for Alpine soils only) and soil horizon using the function *anosim* from the package vegan. Analysis of variance using distance matrices was performed on all samples grouped by, sample site and soil horizon using the *adonis* function from the package vegan with 9999 permutations. Taxa and functions whose abundances differed significantly between horizons depths were identified by applying the Kruskal–Wallis H test (Kruskal and Wallis, 1952) using the function *kruskal.test*, p-values were adjusted for multiple testing using the Benjamin-Hochberg false discovery rate method (Benjamini and Hochberg, 1995) with the function *p.adjust*, only taxa with an adjusted p-value < 0.05 were considered significant.

Data availability

Raw Sequence data files are available in the NCBI sequence read archive under Bioproject number PRJNA39461.

4 RESULTS

DNA EXTRACTION, SEQUENCING DATA QC AND PROCESSING

Vertical sections of weathered sediment (paleosols) in a series of five moraines in the Guil river valley of the French Alps, (G1, G2, G3a, G9, and G11) were sampled at three discrete stratified soil horizons (Ah, Bw and Cox) and were classified as previously described (Mahaney et al., 2016; 2017) (**Figure 1**). The geology of these paleosols is an active area of glacial, cosmic and microbiological research as described in several related geological papers to date (Mahaney et al., 2013, 2016, 2017; Mahaney and Keiser, 2013).

Total DNA per gram of soil generally decreased with increasing depth, indicating a lower total biomass at lower depths in the soil profile (supplementary table S3). Average sequence read lengths were as expected (300bp), average sequence quality was found to be > 20 for the full length of each read for all samples. Adapter contamination was also found to be low, on average < 1% per library. Although merging of the paired end reads was attempted, on average < 30% of reads could be merged, indicating that the average insert size of the sequencing libraries exceeded 600bp, therefore downstream processing was performed on interleaved PE reads.

Attempts at assembly of the metagenomic libraries revealed generally poor assemblies (supplementary table S4) and a significant loss of information (i.e. the percentage of raw reads which could be mapped onto the assembly). Since the goal here was to characterize these soil samples in a general sense it was decided that the loss of information during assembly and

overall poor assembly statistics were deemed unacceptable. Therefore annotation was performed using only the raw PE read files, since the reads were on average 300bp in length, a reasonable level of taxonomic resolution can still be obtained, and in most cases assignments could be made down to the genus level without much further loss of information **(supplementary figure S1).**

On average ~ 80% of all reads could be assigned to at least the Phylum level, the functional gene assignment rates were significantly lower at ranging from 17-26% depending on the SEED subsystem level used. As taxonomic resolution increases so the number of reads which can be confidently assigned to a taxon decreases, with a significant drop-off in the number of reads which can be assigned to the species level, therefor for downstream analysis, the genus level was the minimum taxonomic rank which was analysed..

TAXONOMIC / FUNCTIONAL ANNOTATION

At the class level it is apparent that the community is dominated by four major taxa (**Figure 2**), the *Actinobacteria*, *Alphaproteobacteria*, *Betaproteobacteria* and *Gammaproteobacteria* all of which are common genera of soil microbes which appear to be ubiquitous in soils (Barberán *et al.*, 2014). The Actinobacteria account for roughly 30% of the total annotated reads in all samples. The *Bacilli* and *Acidobacteriia* also appear to be reasonably abundant, as might be expected for paleosols with low pH 4.0-6.0. Certain horizon dependent patterns in the data also emerge even in these boxplots, for example, the *Betaproteobacteria* and *Gammaproteobacteria* appear to be generally more abundant in the Bw and Cox horizon samples while the *Ktedonobacteria* appear to be generally more abundant in the Ah horizon samples.

Alpha / Beta Diversity Analysis

Alpha diversity was estimated for each sample at each taxonomic level using the Shannon–Weaver diversity index (Shannon and Weaver, 1964), Inverse Simpson diversity index (Simpson, 1949) and genus-level richness (i.e. number of unique genera per sample). Linear regression of alpha diversity measures against sample depth reveals a fairly strong, statistically significant linear relationship between soil depth and alpha diversity (**Figure 3**). Interestingly while richness appears to decrease with depth, the diversity indices appear to increase. Both inverse Simpson and Shannon diversity indices account for taxon abundances, where a lower value indicates more uneven taxon abundances, suggesting that while the number of unique genera decrease while moving down a soil profile, the relative abundances of these genera become more even.

In order to test the statistical significance of differences in community structure between horizons, ANOSIM (Figure 3) and Adonis tests (supplementary table S2) were applied. It was necessary to test for homogeneity of group dispersions, i.e. whether or not the multivariate spread of the samples from their group centroids are significantly different (**Figure 3 panel B**). Homogeneity of group dispersion tests were performed for samples grouped by both soil horizon and sample site, results were not statistically significant in any case, meaning that downstream ANOSIM tests may be interpreted confidently without any caveats. The results of both ANOSIM and Adonis tests indicate that soil horizon has a much stronger effect on microbial community than sampling site: the ADONIS R statistic is reasonably high for all ranks when grouped by soil horizon and much lower when grouped by sampling site, indicating that the effect is genuine. Statistical significance is strong with all ranks showing three star significance ($P < 0.001$) when grouped by soil horizon, apart from the phylum level which

shows two star significance ($P < 0.01$) (supplementary table S3). When grouped by sampling site, there is a marginally significant effect at the phylum level although this is not seen at lower levels of taxonomic resolution, or at the functional gene level.

Correlations with Soil Abiotic Variables

The effect of soil horizon classification on soil abiotic variables was also assessed (**Figure 4**). Out of the 27 variables which were assessed here [supplementary data file 1], 12 were found to correlate significantly with soil depth and between stratified soil horizons. These 12 include 5 of the 6 essential elements for life (C, H, N, P, S), it can also be presumed that available oxygen also decreases with soil depth. Where C,N and P were compered total rather than soluble levels were used, because we wanted to consider insoluble sources of these elements (e.g. lignin). Given this information, it is unsurprising that the total DNA per g of soil decreases with depth and that the microbial communities between soil horizons are significantly different from one another (ANOSIM significance = $3.9e^{-4}$) (**Figure 3**). Conversely, the concentration of numerous elements important for life (Ca, Cu, Na, K and Mn) appears to increase with soil depth – perhaps due to leaching. This is typical during weathering of parent material, when the elements are realised they are leached down profile (Retallack, 2001). The exception is K that follows decreasing trend toward the parent rock. The K is most likely incorporated into secondary clay minerals like Illite, illite-smectite and/or illite-vermiculite (Mahaney et al., 2016).

Principal Component Analysis

Principle component analysis was performed on taxon abundances (at the class and genus levels), functional abundances (at SEED subsystems level 1) and abiotic variables (**Figure 5**),

revealing strikingly similar patterns between samples in multivariate space. There is a clear and consistent separation of soil horizons along the first principal component axis in all cases. There is also a slight overlap between Bw and Cox horizons in the case of the Genus level abundance and chemical variables, indicating that the Bw and Cox horizons are less strongly differentiated from each other. This corresponds with the sedimentology - which indicates that the Bw horizon is only weakly differentiated and still developing (hence the w classification), and therefore it is not surprising that these data suggest a closer degree of similarity between population in the Bw and Cox horizons (Mahaney *et al.*, 2013). In all cases, the first two principle component axes cumulatively explain > 70% of the total variation (> 80% in the case of the taxonomic variation).

In order to identify the taxa and functions which contribute most to the differences between soil horizons the Kruskal-Wallace H test (Kruskal and Wallis, 1952) for differences between groups was applied to taxonomic abundances at the class level, and functional abundances at level 1 Of the SEED subsystems hierarchy. For clarity, plots were only produced for taxa and functions which occurred at an abundance greater than 0.1% in at least one sample.

It is clear that the abundances of many classes of bacteria vary along the depth profile (**Figure 6**). Nine of the top ten most significantly variable taxa appear to increase with soil depth, while the only one which decreases are the *Ktedonobacteria.* Likewise, classes which are known to comprise many obligate and facultative anaerobes (the *Bacilli*, *Clostridia* and *Negativicutes*) increase significantly with depth. The *Betaproteobacteria* are one of the most abundant classes present in the dataset and show a near 3% increase in median abundance between the Ah and Cox horizons. A total of 57 Classes were shown to vary significantly between soil horizons, applying this analysis to genus level abundances revealed that 1223

genera vary significantly between soil horizons. Overall, what has become clear from these data is that a large number taxa vary significantly and consistently between soil horizons over all six sample sites, even when measured at higher taxonomic ranks.

Similarly, many functional gene categories vary in abundance with respect to soil horizon, although the effect is much less pronounced than for taxon abundances, with only 6 major categories showing significant variation (**Figure 7**). Nitrogen metabolism and carbohydrate metabolism are the two which can be most obviously linked to ecosystem level processes. Both decrease with increasing depth, corresponding to the decrease in soil nitrogen and organic carbon with depth recorded by Mahaney, et al. (2016). The low measured N (supplementary data file 1) concentrations in these soils would suggest that the environment is extremely nitrogen limited. Therefore we would expect that Ammonia oxidation may be an extremely important component of the nitrogen cycle in these soils. Genes relating to central metabolism (i.e. metabolic pathways essential for organism survival) and secondary metabolism (i.e. pathways which are non-essential) show a near inverse relationship, with secondary metabolism decreasing with depth while central metabolism genes increase with depth. This may be explained by the fact that in lower soil horizons, where nutrients are less abundant (Fierer, 2017), functions which are non-essential for survival are less vital and thus are selected against over time - core metabolism genes become more important.

Additionally, in the Ah horizon where C N and P are more abundant we might expect anti-microbial secondary metabolites biosynthesis genes to be more prevalent due to the higher abundance of microbes competing for these nutrients. In lower soil horizons with less microbial activity, competition for nutrients is likely to be lower leading to a drop in the

346 abundance of anti-microbial biosynthesis genes, although this cannot be confirmed from the
347 results of this study. This does however suggest the possibility that nutrient-rich surface soil
348 horizons may be ideal locations to screen for the presence of novel antimicrobial compounds
349 and future work should endeavour to test this hypothesis. Fatty acid and isoprenoid synthesis
350 genes are more abundant in the Ah horizon, this may be due to the fact these genes are
351 heavily involved in cell membrane maintenance and manufacture (Kaneda, 1991), and may
352 indicate that the Ah horizon hosts the most actively growing microbial cells. Finally,
353 membrane transport related genes appear to be most abundant in the Cox horizons. The
354 reason for this trend is not immediately obvious, though one could speculate that it may be
355 connected to an increase in chemo-lithotrophic lifestyles in the lower mineral soil horizons –
356 where alternative electron donors (such as sulfide, ferric Iron or ammonia) must be
357 transported across the cell membrane before they can be used by the cell for ATP synthesis
358 (Peck 2003).

359 Carbohydrate metabolism is one of the largest SEED subsystem categories and contains many
360 subcategories of genes which are linked to the carbon cycle, therefore carbohydrate
361 metabolism genes were analyzed in more detail (**Figure 8**). After multiple test corrections
362 were applied 5 categories within carbohydrate metabolism show significant variation. Poly,
363 mono, di and oligo saccharide metabolism genes all decrease moving down the soil profile, as
364 do carbon dioxide fixation genes. This is hardly surprising due to the fact that organic carbon,
365 and carbon dioxide are generally present at higher concentrations in upper soil horizons.
366 However, one-carbon metabolism genes appear to increase with soil depth, as might be
367 expected given the importance of the methane cycle in low organic carbon environments
368 (Serrano-Silva *et al.*, 2014). A picture of the carbon cycle in these soils then begins to emerge
369 whereby organic carbon is primary energy and provides carbon sources for many microbes in

upper soil horizons as might be expected, while organisms in lower soil horizons gain energy and carbon by utilizing reduced one-carbon compounds (e.g. methane) as energy sources which are liberated from the anaerobic turnover of waste products from the upper horizons.

5 Discussion

It is clear that the abundances of many bacterial vary consistently between stratified soil horizons (Figure 6). We found that the *Ktedonobacter* showed the largest differential abundance between stratified soil horizon and was generally most abundant in the Ah horizons, members of this class are thought to be aerobic filamentous, spore-forming, gram-positive, heterotrophic bacteria (Yabe et al. 2017). Conversely, many classes of obligate and facultative anaerobes decreased in abundance with soil depth (eg. the *Bacilli*, *Clastridiales*) (Figure 3), suggesting a strong influence of oxygen availability on the community composition. Interestingly, the most abundant classes of microbes across all samples (eg: *Acinobacteria*, *Proteobacteria*) (Figure 2) did not show a statistically significant variation in abundance between soil horizons (Figure 6), perhaps suggesting that the more successful microbes in these environments are ones with mixotrophic lifestyles who can adapt to variable conditions between soil horizons.

When comparing functional profiles between soil horizons, differences in certain biogeochemical cycling genes become clear. It is evident that many gene abundances correlate either positively or negatively with depth, which is understandable given that most key nutrients will vary down profile. Nitrogen metabolism appears to decrease with increasing depth, and likewise, carbohydrate metabolism genes appear to be significantly

more abundant in the Ah horizon, corresponding to the zone of highest organic carbon turnover (evident from CNP measurements, Mahaney et al., 2016). Taking a more detailed look at carbohydrate metabolism (**Figure 8**) revealed that there are significant variations even within this category. Carbon dioxide (autotrophy) and central carbohydrate metabolism genes appear to be relatively abundant in the Ah horizon, while genes for other one-carbon metabolism becomes more abundant in the Cox horizon. This is consistent with increasing abundance of methane (associated with both methylotrophy and methanogenesis) turnover processes in deeper soils (Dunfield, 2007). This is likely due to the fact that, as complex plant polymers are broken down by microbes in the upper soil horizons, reduced carbon compounds are produced as waste products and filter down to the lower horizons where they are then utilized by methylotrophic microbes.

It should be noted that there is significant co-linearity between the many abiotic and biotic variables measured and compared here. As an example, looking specifically at almost all other abiotic and biotic parameters correlate with soil depth (in cm) to some degree (Figure 5). Therefore it was not possible to investigate and compare correlations between individual taxa/functions and abiotic variables as disentangling this co-linearity to reveal the true source of variation is not possible without carefully designed laboratory experiments to control for the effect of specific co-linear variables identified here. Indeed, any attempt to do so may be statistically dubious and may therefore be considered as an example of “p-hacking” (Head *et al.*, 2015). However, this analysis makes it abundantly clear that soil horizon matters: in terms of chemistry, taxonomy and functionality of the community.

There are several important caveats to the results presented here that must also be considered. Firstly, metagenomes are not expected to be static over time, so caution must be taken when making broad statements about a microbial community. In extreme cases, we might expect drastic changes in microbial community structure to (Mahaney et al., 2017). Otherwise, previous studies have established that temporal variation within soil microbiomes is generally much lower than spatial variation (Lauber *et al.*, 2013), so the patterns observed here are likely to persist across seasons, at least in the short term. Secondly, for any enzyme-catalysed processes to occur, transcription and translation of protein coding genes are essential requirements. Therefore, a positive relationship between the abundance of gene or transcripts and corresponding process rate is not always necessarily true, though it is often presumed. Rocca *et al.*, (2015) indicated that functional gene abundances are only weakly correlated to process rates, but are consistently correlated across multiple environments. Finally, the relatively low depth of sequencing per sample means that complete genomes cannot be resolved, (a common limitation for diverse soil metagenomes (Nesme et al. 2016) and annotations are based on ~300bp fragments. Much more robust results could be obtained with more complete genomes and functional genes, allowing investigation of functional genes in their genomic context, and analysis of complete metabolic pathways within certain species. The relatively short read length used here may be useful for taxonomic classification but full length genes are preferable for functional annotation. Despite this limitation, there is a growing body of evidence to suggest that shallower sequencing across many samples with suitable replication levels is sufficient to answer key questions about microbial ecology (Knight *et al.*, 2012).

Fundamentally we know that soil stratigraphy is a function of soil chemistry (USDA 1999). Our full metagenome data, for the first time, show that soil stratigraphy is strongly correlated with variation in microbial community composition – as shown in figures 3 and 5. Furthermore we find that the variation seen between stratified soil horizons is greater than the variation seen between soil sampling sites when taken as a whole (Figure 3).

Ultimately, the physical and chemical properties of a soil are the true drivers of microbial diversity and soil horizons are a useful method for categorizing soils with similar physicochemical characteristics. While the gene analysis presented here has provided an overview of microbial community structure and functionality in alpine soils, it has also highlighted a need for more specific methods in order to make definitive statements about biogeochemical processes occurring between soil horizons. The use of more specific and informative functional gene ontologies or the use of meta-transcriptomic information will certainly add a further level of understanding to this field. One correlation that we did not investigate in this study, is the relationship between oxygen concentration and/or redox potential with metagenome composition down profile. In general we would expect these to decrease with depth. Clearly there is abundant microbial activity in the sediments, and oxygen – as the ultimate acceptor – would certainly become limiting to microbial metabolism within a cm or two of the Ah horizon (Birkeland, 1999).

CONCLUSION

In conclusion, our study begins to demonstrate a clear relationship between the physico-chemical parameters that are typically used to define soil pedons, and parallel the structure of complex microbial communities. The ability to do so has only become available to us in

recent years due to the advent of shotgun sequencing and metagenomic analysis. The limitations of culture-dependant microbial analysis, have previously not allowed any such connection to be established. However, in this study some dependency is evident: the reduction between organic carbon availability and the related genetic profile of functional genes involved in C1 turnover is especially clear and is quite rational. The results here may lead us to consider that the formation of paleosol horizons is inextricably linked to the biological, not just physical and chemical transformations that occur. Critically, we emphasise here a key finding in this study – that variation in microbial gene populations between palesol samples sites, sometimes hundreds of metres apart, is significantly less than that seen between soil pedons, just centimetres apart at specific sample sites. This remarkable metagenome diversity may be exploited for gene mining applications.

Acknowledgements

We acknowledge the REMEDIATE KTN (CCRA, BK), Invest Northern Ireland (TS), and Quaternary Surveys (WM) for financial support.

6 REFERENCES

Andrews S. (2010). FastQC: a quality control tool for high throughput sequence data. http://www.bioinformatics.babraham.ac.uk/projects/fastqc.¶

Baldrian P, Kolařík M, Štursová M, Kopecký J, Valášková V, Větrovský T, et al. (2012). Active and total microbial communities in forest soil are largely different and highly stratified during decomposition. ISME J 6: 248–258.¶

485 Bankevich A, Nurk S, Antipov D, Gurevich AA, Dvorkin M, Kulikov AS, et al. (2012). SPAdes: A New
486 Genome Assembly Algorithm and Its Applications to Single-Cell Sequencing. J Comput Biol 19: 455–
487 477.¶

488

489 Barberán A, Ramirez KS, Leff JW, Bradford MA, Wall DH, Fierer N. (2014). Why are some microbes
490 more ubiquitous than others? Predicting the habitat breadth of soil bacteria. Ecol Lett 17: 794–802.¶

491

492 Birkeland, P.W., 1999. Soils and Geomorphology. Oxford University Press, Oxford, UK, p. 430.¶

493

494 Bushnell B. (2015). BBMap short-read aligner, and other bioinformatics tools. Available from
495 sourceforge net/projects/bbmap.¶

496

497 Byers AC. (2008). An assessment of contemporary glacier fluctuations in Nepal's Khumbu Himal
498 using repeat photography. Himal J Sci 4: 21-26.¶

499

500 Canada Soil Survey Committee (CSSC), (1998). The Canadian System of Soil Classification, 637. NRC
501 Research Press, Ottawa, Canada, p. 187.¶

502

503 Clarke KR. (1993). Non-parametric multivariate analyses of changes in community structure. Austral
504 Ecol 18: 117–143. ¶

505

506 Davidson EA, Janssens IA. (2006). Temperature sensitivity of soil carbon decomposition and
507 feedbacks to climate change. Nature 440: 165–173.¶

508

509 Ding J, Zhang Y, Deng Y, Cong J, Lu H, Sun X, et al. (2015). Integrated metagenomics and network
510 analysis of soil microbial community of the forest timberline. Sci Rep 5: 7994.¶

511

512 Dunfield, PF. (2007). 10 The Soil Methane Sink. Greenhouse gas sinks, p.152.¶

513

514 Fierer N, Strickland MS, Liptzin D, Bradford MA, & Cleveland CC. 2009. Global Patterns in
515 Belowground Communities. Ecology Letters 12: 1238–49.¶

516

517 Fierer N. (2017). Embracing the unknown: disentangling the complexities of the soil microbiome. Nat
518 Rev Microbiol 15: 579–590.¶

519 Head ML, Holman L, Lanfear R, Kahn AT, Jennions MD. (2015). The extent and consequences of p-
520 hacking in science. PLoS Biol 13: e1002106.¶

521

522 He S, Wurtzel O, Singh K, Froula JL, Yilmaz S, Tringe SG, et al. (2010). Validation of two ribosomal
523 RNA removal methods for microbial metatranscriptomics. Nat Methods 7: 807– 812.¶

524

525 Hodgson, JM. (1976). Soil Survey Field Handbook d Soil Survey Tech, Monograph, No. 5. 773.
526 Rothamsted Experimental Stn, Harpenden, Herts, p. 99.¶

527

528 Huson DH, Beier S, Flade I, Górska A, El-Hadidi M, Mitra S, et al. (2016). MEGAN Community Edition -
529 Interactive Exploration and Analysis of Large-Scale Microbiome Sequencing Data. PLOS Comput Biol
530 12: e1004957.¶

531

532 Kaneda T. (1991). Iso- and anteiso-fatty acids in bacteria: biosynthesis, function, and taxonomic
533 significance. Microbiol Rev 55: 288–302.¶

534

535 King AJ, Karki D, Nagy L, Racoviteanu A, Schmidt SK. (2011). Microbial biomass and activity in high
536 elevation (> 5100 meters) soils from the Annapurna and Sagarmatha regions of the Nepalese
537 Himalayas. Himal J Sci 6: 11-18¶

538

539 Knight R, Jansson J, Field D, Fierer N, Desai N, Fuhrman JA, et al. (2012). Unlocking the potential of
540 metagenomics through replicated experimental design. Nat Biotechnol 30: 513–20.¶

541

542 Körner, Christian, and Jens Paulsen. (2004). A World-Wide Study of High Altitude Treeline
543 Temperatures. Journal of Biogeography 31: 713–32.¶

544

545 Kruskal WH, Wallis WA. (1952). Use of ranks in one-criterion variance analysis. J Am Stat Assoc 47:
546 583–621.¶

547

548 Lal, R. (2004). Soil carbon sequestration impacts on global climate change and food security. Science
549 304: 1623-1627.

550

551 Lauber CL, Ramirez KS, Aanderud Z, Lennon J, Fierer N. (2013). Temporal variability in soil microbial
552 communities across land-use types. ISME J 7: 1641–1650.¶

553

554 Lazzaro A, Hilfiker D, Zeyer J. (2015). Structures of Microbial Communities in Alpine Soils: Seasonal
555 and Elevational Effects. Front Microbiol 6: 1330.¶

556

557 Legendre P, Gallagher ED. (2001). Ecologically meaningful transformations for ordination of species
558 data. Oecologia 129: 271–280.¶

559

560 Li D, Luo R, Liu CM, Leung CM, Ting HF, Sadakane K, Yamashita H, Lam TW. (2016). MEGAHIT v1. 0: A
561 fast and scalable metagenome assembler driven by advanced methodologies and community
562 practices. Methods102: 3-11.

563

564 Mahaney WC, Keiser L. (2013). Weathering rinds-unlikely host clasts for an impact- induced event.
565 Geomorphology 184: 74-83¶

566

567 Mahaney, WC, Somelar, P, West A, Krinsley D, Allen CCR, Pentlavalli P, Young JM, Dohm JM,
568 LeCompte M, Kelleher B, Sean J, Pulleyblank C, Dirszowsky R, Costa P. (2017) Evidence for cosmic
569 airburst/impact in the Western Alps archived in Late Glacial Paleosols. Quaternary International,
570 438: 68-80.¶

571

572 Mahaney WC, Keiser L, Krinsley DH, Pentlavalli P, Allen CCR, Somelar P, et al. (2013). Weathering
573 rinds as mirror images of paleosols: examples from the Western Alps with correlation to Antarctica
574 and Mars. J Geol Soc London 2012: 150.

575

576

577 Mahaney WC, Somelar P, Dirszowsky RW, Kelleher B, Pentlavalli P, McLaughlin S, et al. (2016). A
578 Microbial Link to Weathering of Postglacial Rocks and Sediments, Mount Viso Area, Western Alps,
579 Demonstrated through Analysis of a Soil/Paleosol Bio/Chronosequence. Journal of Geology. 124:
580 149–169.¶

581

582 Menzel P, Ng KL, Krogh A, Marth G, Lipman D. (2016). Fast and sensitive taxonomic classification for
583 metagenomics with Kaiju. Nat Commun 7: 11257.¶

584

585 Mitra S, Rupek P, Richter DC, Urich T, Gilbert JA, Meyer F, Wilke A, Huson DH. (2011) Functional
586 analysis of metagenomes and metatranscriptomes using SEED and KEGG. BMC bioinformatics. 12:
587 S21.

588

589 National Soil Survey Center (NSSC), 1995. Soil Survey Laboratory Information Manual. Soil Survey
590 Investigations Report No. 45. Version 1.00. USDA, Washington, DC., p. 305¶

NCBI Resource Coordinators. (2017). Database Resources of the National Center for Biotechnology Information. Nucleic Acids Res 45: D12–D17.¶

Neira, J., Ortiz, M., Morales, L., & Acevedo, E. (2015). Oxygen diffusion in soils: Understanding the factors and processes needed for modeling. Chilean journal of agricultural research 75: 35-44.¶

Nesme J, Achouak W, Agathos SN, Bailey M, Baldrian P, Brunel D, et al. (2016). Back to the Future of Soil Metagenomics. Front Microbiol 7: 73.¶

Oksanen J, Blanchet FG, Kindt R, Legendre P, Minchin PR, O'hara RB, Simpson GL, Solymos P, Stevens MH, Wagner H (2011). vegan: Community ecology package. R package version. 2011:117-8.

Overbeek R, Begley T, Butler RM, Choudhuri J V, Chuang H-Y, Cohoon M, et al. (2005). The Subsystems Approach to Genome Annotation and its Use in the Project to Annotate 1000 Genomes. Nucleic Acids Res 33: 5691–5702.¶

Oyama, M., Takehara, H., (1970). Standard Soil Color Charts. Japan Research Council for Agriculture, Forestry and Fisheries, Tokyo, Japan.

Peck Jr, H. D. (1968). Energy-coupling mechanisms in chemolithotrophic bacteria. Annual Reviews in Microbiology 22: 489-518.¶

Peng Y, Leung HCM, Yiu SM, Chin FYL. (2012). IDBA-UD: a de novo assembler for single-cell and metagenomic sequencing data with highly uneven depth. Bioinformatics 28: 1420–1428.¶

Quast C, Pruesse E, Yilmaz P, Gerken J, Schweer T, Yarza P, et al. (2013). The SILVA ribosomal RNA gene database project: improved data processing and web-based tools. Nucleic Acids Res 41: D590–D596.¶

R Core Team. (2011). R: A Language and Environment for Statistical Computing. R Found Stat Comput 1: 409.¶

Retallack GJ, (2001). Soils of The Past: An Introduction to Paleopedology, 2nd ed., Blackwell, Oxford, UK. 600 p.

627 Rocca JD, Hall EK, Lennon JT, Evans SE, Waldrop MP, Cotner JB, et al. (2015). Relationships between
628 protein-encoding gene abundance and corresponding process are commonly assumed yet rarely
629 observed. ISME J 9: 1693–9.¶

630

631 Serna-Chavez HM, Fierer N, van Bodegom PM. (2013). Global drivers and patterns of microbial
632 abundance in soil. Glob Ecol Biogeogr 22: 1162–1172.¶

633

634 Serrano-Silva N, Sarria-Guzan Y, Dendooven L, Luna-Guido M. (2014). Methanogenesis and
635 Methanotrophy in Soil: A Review. Pedosphere 24: 291–307.¶

636

637 Shannon CE, Weaver W. (1964). The mathematical theory of communication. University of Illinois
638 Press.¶

639

640 Simpson, E.H. (1949). Measurement of diversity. Nature.¶

641

642 Tukey JW (John W. (1977). Exploratory data analysis. Addison-Wesley Pub. Co.¶

643

644 USDA. (1999). Soil taxonomy: A basic system of soil classification for making and interpreting soil
645 surveys. 2nd edition.¶

646 Weigold P, El-Hadidi M, Ruecker A, Huson DH, Scholten T, Jochmann M, et al. (2016). A
647 metagenomic-based survey of microbial (de)halogenation potential in a German forest soil. Sci Rep
648 6: 28958.¶

649

650 Yabe S, Sakai Y, Abe K, Yokota A. (2017). Diversity of Ktedonobacteria with Actinomycetes- Like
651 Morphology in Terrestrial Environments. Microbes Env 32: 61–70.¶

652

653 Yashiro E, Pinto-Figueroa E, Buri A, Spangenberg JE, Adatte T, Niculita-Hirzel H, et al. (2016). Local
654 Environmental Factors Drive Divergent Grassland Soil Bacterial Communities in the Western Swiss
655 Alps. Appl Environ Microbiol 82: 6303–6316.¶

656

657 Yu, K., Faulkner, S. P., & Patrick Jr, W. H. (2006). Redox potential characterization and soil
658 greenhouse gas concentration across a hydrological gradient in a Gulf coast forest. Chemosphere 62:
659 905-914.¶

660

661 Zemp M, Haeberli W, Hoelzle M, Paul F. (2006). Alpine glaciers to disappear within decades?
662 Geophys Res Lett 33: L13504¶

Zhang Y, Lu Z, Liu S, Yang Y, He Z, Ren Z, et al. (2013). Geochip-based analysis of microbial communities in alpine meadow soils in the Qinghai-Tibetan plateau. BMC Microbiol 13: 72.¶

FIGURE LEGENDS

Figure 1: Overview of Sampling sites and soil stratigraphy. Panel A: Satellite map of sampling area. Panel B: Stratigraphy of soil profiles for each sample (from Mahaney *et al*., 2016). Sampling sites are shown at the top of each profiles, depth in centimeters is displayed on the left and soil horizon classification is displayed on the right of each profile.

Figure 2: Boxplot showing the relative abundances of the 20 most abundant Taxa across all samples at the Class level. Jittered points overlaid on boxplots represent individual sample and are coloured by sample soil horizon classification. The bottom and top of the boxes represent the first and third quartiles, with the central band representing the median, whiskers represent 1.5 times the interquartile range according to Tukey's schematic boxplot method (Tukey, 1977)

Figure 3: Diversity analysis of alpine soils. **Panel A:** Alpha diversity plots for taxonomic abundance tables at each taxonomic level. Y axis represents inverse Simpson diversity index, Shannon-Weaver diversity index, and Genus level richness (i.e. the number of unique genera detected per sample) respectively. X axis represents depth in cm of soil sample. Blue lines represent linear regressions, shaded area represents the 95% confidence interval for the regression analysis. R^2 values and P-values for linear regressions along with significance codes are displayed for each plot. **Panel B:** homogeneity of group dispersions for samples grouped by soil horizon, Y axis represents distance to the group centroid in 2d Euclidean space, standard error of the mean across all samples, analysis of variance (ANOVA) test P

687 value for differences between soil horizons value is displayed on the plot. Panel C: Boxplot
688 of analysis of similarities (ANOSIM) results, Y axis represents ranked order of dissimilarities
689 ANOSIM R statistic and significance level are shown on the plot, significance of the R statistic
690 was assessed by permutation for 9999 replicates. The bottom and top of the boxes
691 represent the first and third quartiles, with the central band representing the median,
692 whiskers represent 1.5 time the interquartile range according to Tukeys schematic boxplot
693 method (Tukey, 1977).

694 **Figure 4:** Analysis of effect of paleosol depth and paleosol horizon on paleosol abiotic
695 variables. **Panel A:** Spearmans rank correlation matrix for pairwise correlations between soil
696 geochemical variables. Points are coloured and scaled according to the value of the
697 correlation coefficient, only correlations with a P value < 0.05 are displayed. Variables which
698 correlate significantly with soil depth are highlighted in red. **PanelB:** Boxplots of
699 geochemical variables which vary significantly between stratified soil horizons. The bottom
700 and top of the boxes represent the first and third quartiles, with the central band
701 representing the median, whiskers represent 1.5 time the interquartile range according to
702 Tukeys schematic boxplot method (Tukey, 1977).

703 **Figure 5:** PCoA plots of abundance tables at each taxonomic and functional rank. Constrained analysis
704 of principal components was performed on dissimilarity matrices using the function capscale from the
705 package Vegan (Oksanen et al., 2016) in R version 3.4.1 (R Core Team, 2011). In each case the x and y
706 axis represent the first and second principal component axis respectively. Points are coloured by soil
707 horizon and the convex hulls are drawn and highlighted for each horizon grouping.

708 **Figure 6:** Boxplots showing relative abundance of microbial classes which differed significantly
709 between soil horizons. Relative abundance is expressed as a percentage of the total annotated reads.
710 The bottom and top of the boxes represent the first and third quartiles, with the central band

711 representing the median, whiskers represent 1.5 time the interquartile range according to Tukey's
712 boxplot method (Tukey, 1977). All data points are also plotted as points.

713 **Figure 7:** Boxplots of relative abundance of SEED level 1 functional categories. Relative abundance is
714 expressed as a percentage of the total annotated reads. The bottom and top of the boxes represent
715 the first and third quartiles, with the central band representing the median, whiskers represent 1.5
716 times the interquartile range according to Tukey's boxplot method (Tukey, 1977). All data points are
717 also plotted as jittered points.

718 **Figure 8:** Abundance of SEED level 2 categories related to carbon metabolism. Relative abundance is
719 expressed as a percentage of the total annotated reads. The bottom and top of the boxes represent
720 the first and third quartiles, with the central band representing the median, whiskers represent 1.5
721 time the interquartile range according to Tukey's boxplot method (Tukey, 1977). All data points are
722 also plotted as points.

723

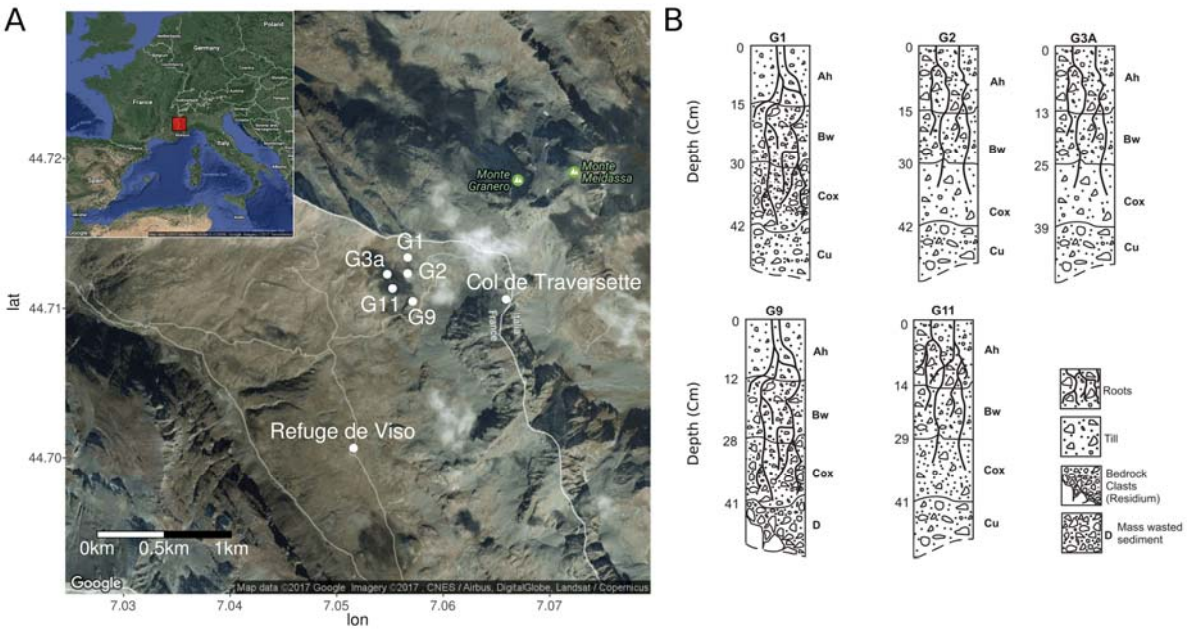

Figure 1: Overview of Sampling sites and soil stratigraphy. Panel A: Satellite map of sampling area. Panel B: Stratigraphy of soil profiles for each sample (from Mahaney *et al.*, 2016). Sampling sites are shown at the top of each profiles, depth in centimetres is displayed on the left and soil horizon classification is displayed on the right of each profile.

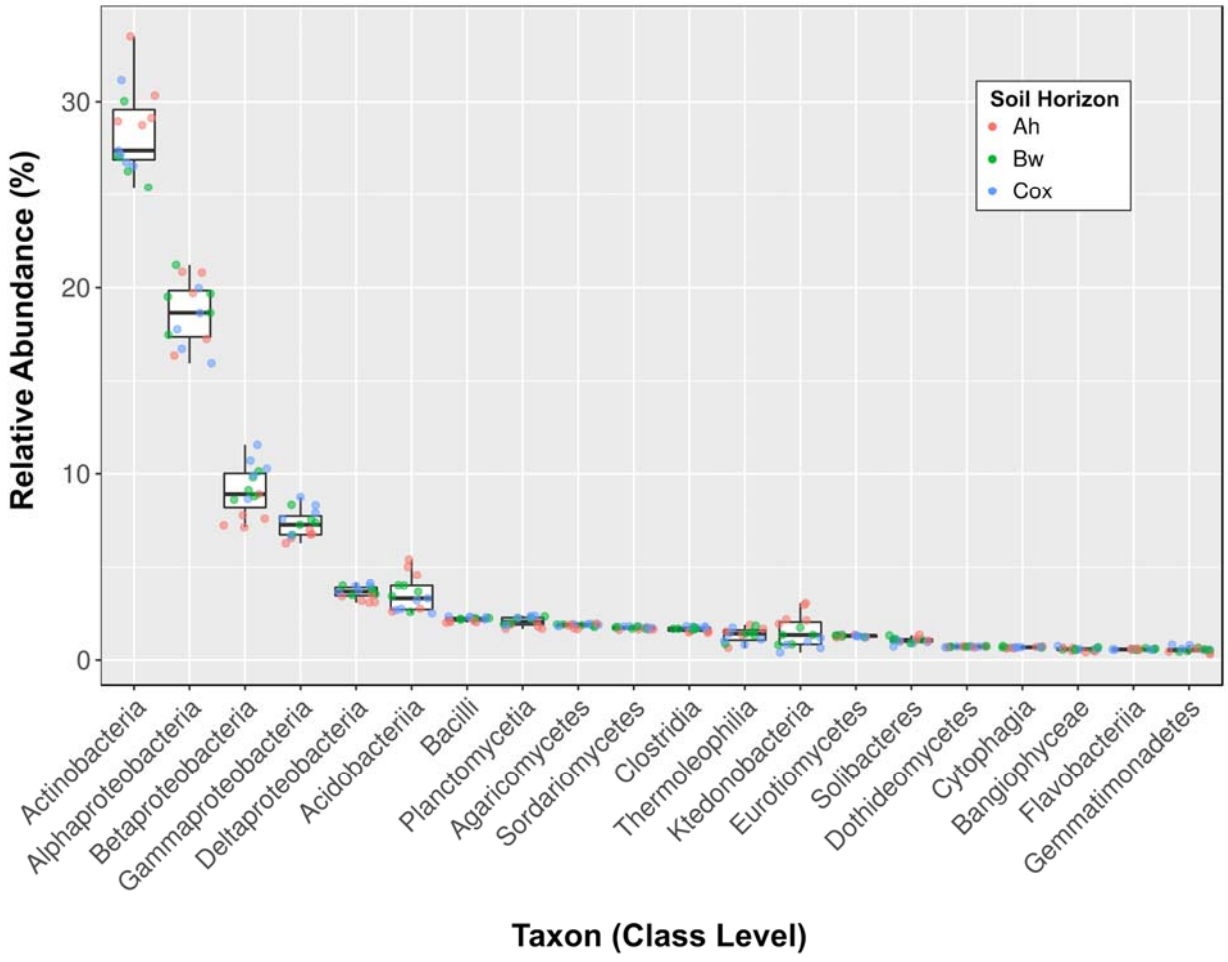

Figure 2: Boxplot showing the relative abundances of the 20 most abundant Taxa across all samples at the Class level. Jittered points overlaid on boxplots represent individual sample and are coloured by sample soil horizon classification. The bottom and top of the boxes represent the first and third quartiles, with the central band representing the median, whiskers represent 1.5 times the interquartile range according to Tukey's schematic boxplot method (Tukey, 1977)

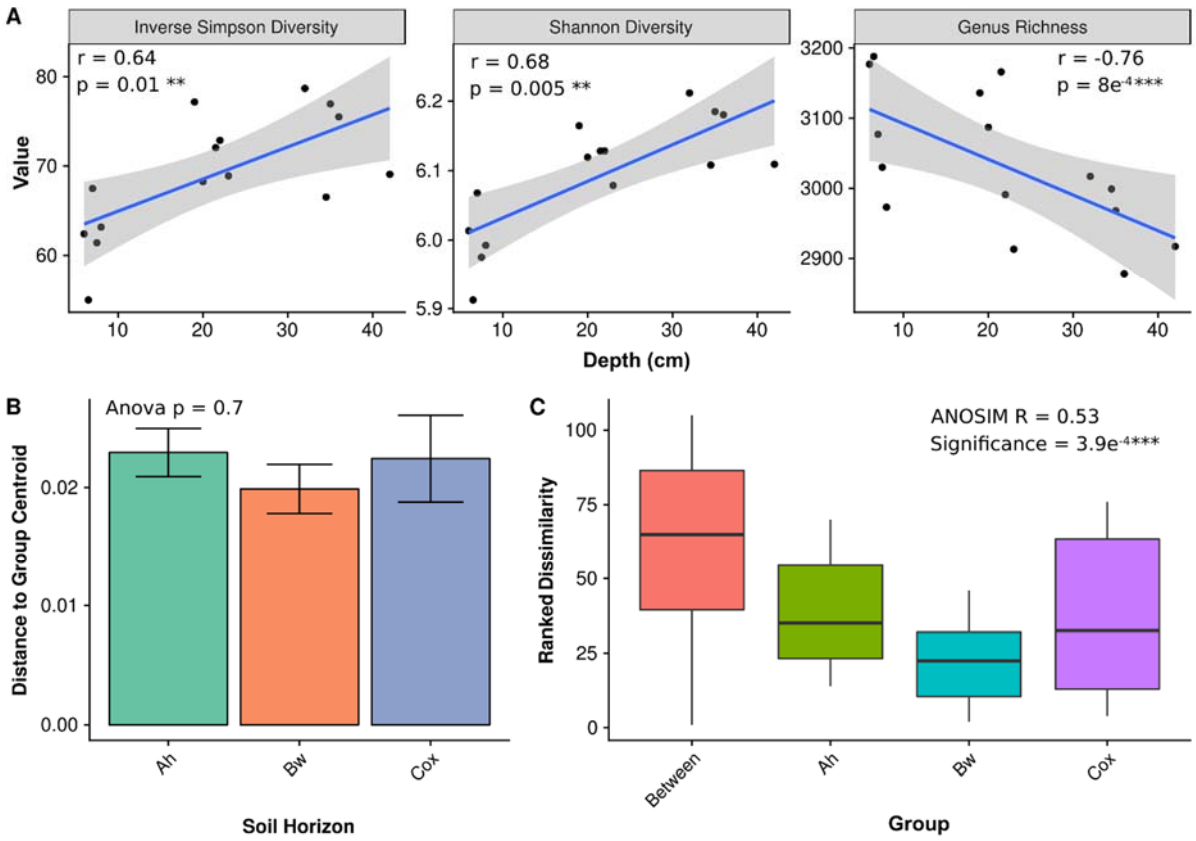

Figure 3: Diversity analysis of alpine soils. **Panel A:** Alpha diversity plots for taxonomic abundance tables at each taxonomic level. Y axis represents inverse Simpson diversity index, Shannon-Weaver diversity index, and Genus level richness (i.e. the number of unique genera detected per sample) respectively. X axis represents depth in cm of soil sample. Blue lines represent linear regressions, shaded area represents the 95% confidence interval for the regression analysis. R^2 values and P-values for linear regressions along with significance codes are displayed for each plot. **Panel B:** homogeneity of group dispersions for samples grouped by soil horizon, Y axis represents distance to the group centroid in 2d Euclidean space, standard error of the mean across all samples, ANOVA test P value for differences between soil Horizons value is displayed on the plot. Panel C: Boxplot of ANOSIM results, Y axis represents ranked order of dissimilarities ANOSIM R statistic and significance level are shown on the plot, significance of the R statistic was assessed by permutation for 9999 replicates. The bottom and top of the boxes represent the first and third quartiles, with the central band representing the median, whiskers represent 1.5 time the interquartile range according to Tukeys schematic boxplot method (Tukey, 1977).

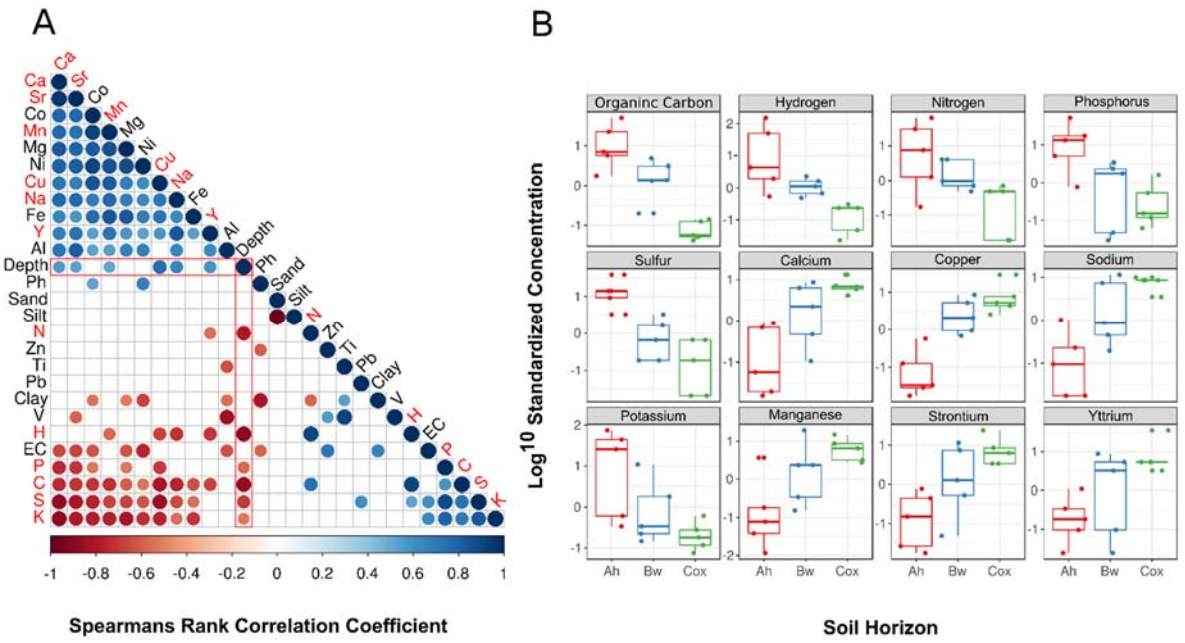

Figure 4: Analysis of effect of paleosol depth and paleosol horizon on paleosol abiotic variables. **Panel A:** Spearmans rank correlation matrix for pairwise correlations between soil geochemical variables. Points are coloured and scaled according to the value of the correlation coefficient, only correlations with a P value < 0.05 are displayed. Variables which correlate significantly with soil depth are highlighted in red. **PanelB:** Boxplots of geochemical variables which vary significantly between stratified soil horizons. The bottom and top of the boxes represent the first and third quartiles, with the central band representing the median, whiskers represent 1.5 time the interquartile range according to Tukeys schematic boxplot method (Tukey, 1977).

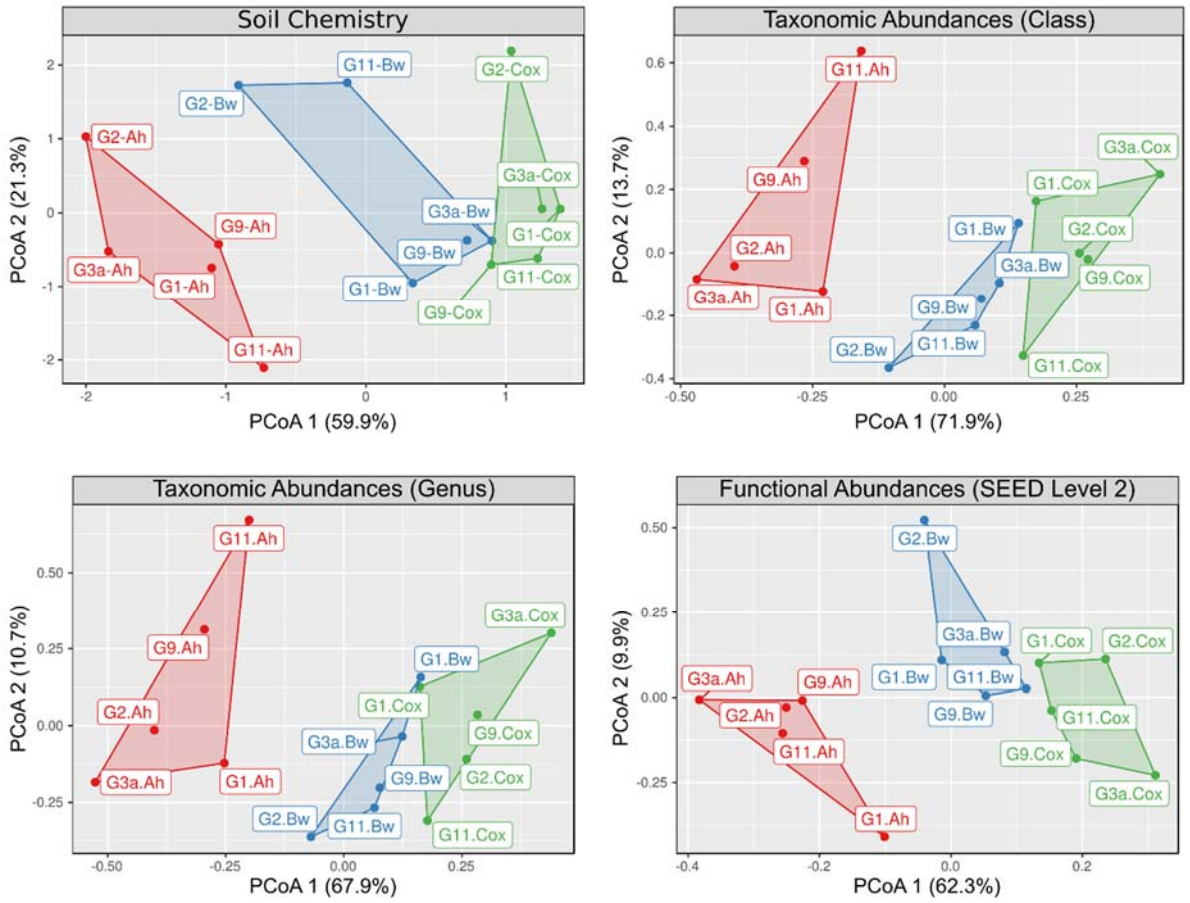

762

763 **Figure 5:** PCoA plots of abundance tables at each taxonomic and functional rank. Constrained analysis
764 of principal components was performed on dissimilarity matrices using the function capscale from the
765 package Vegan (Oksanen et al., 2016) in R version 3.4.1 (R Core Team, 2011). In each case the x and y
766 axis represent the first and second principal component axis respectively. Points are coloured by soil
767 horizon and the convex hulls are drawn and highlighted for each horizon grouping.

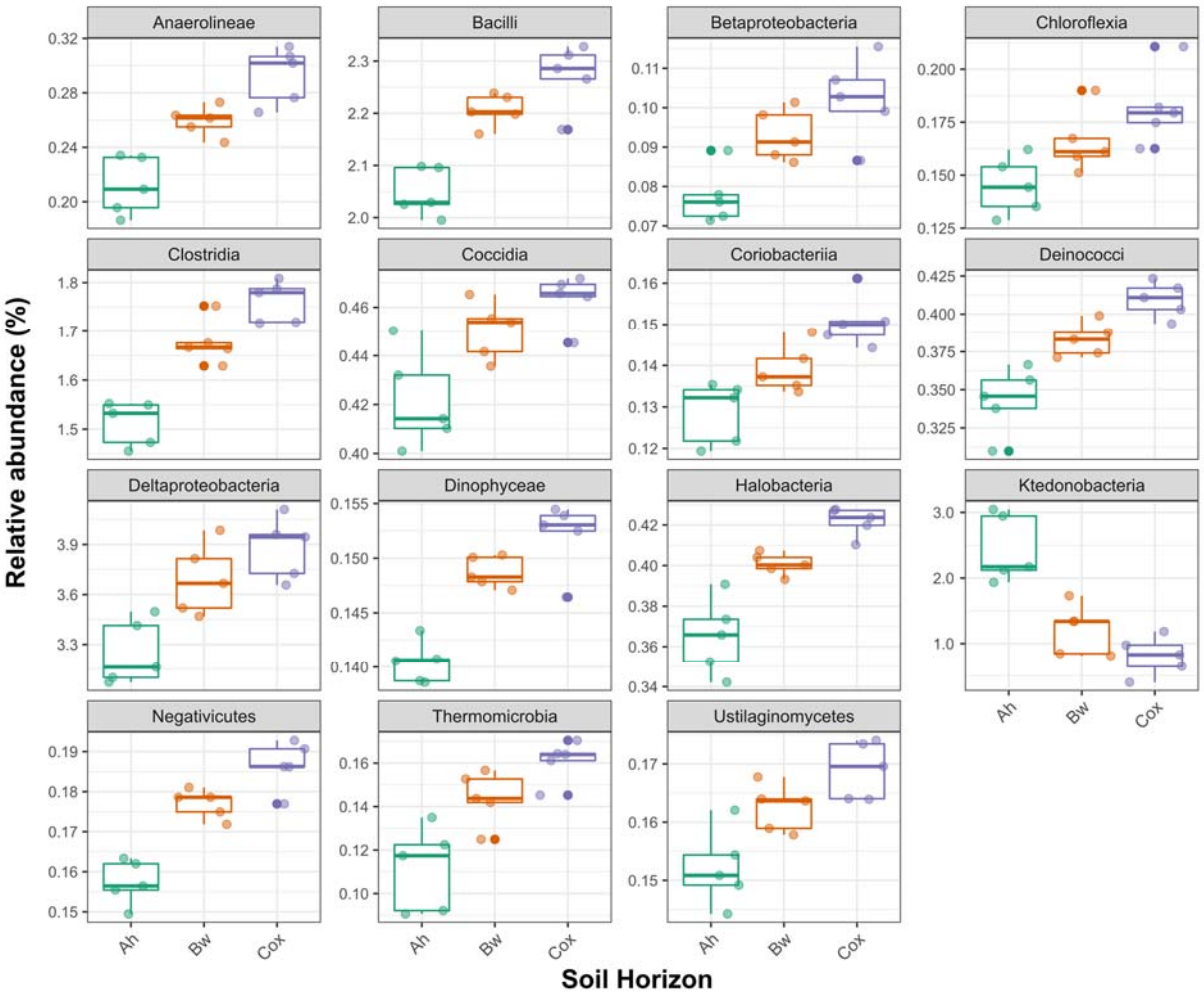

Figure 6: Boxplots showing relative abundance of microbial classes which differed significantly between soil horizons. Relative abundance is expressed as a percentage of the total annotated reads. The bottom and top of the boxes represent the first and third quartiles, with the central band representing the median, whiskers represent 1.5 time the interquartile range according to Tukey's boxplot method (Tukey, 1977). All data points are also plotted as points.

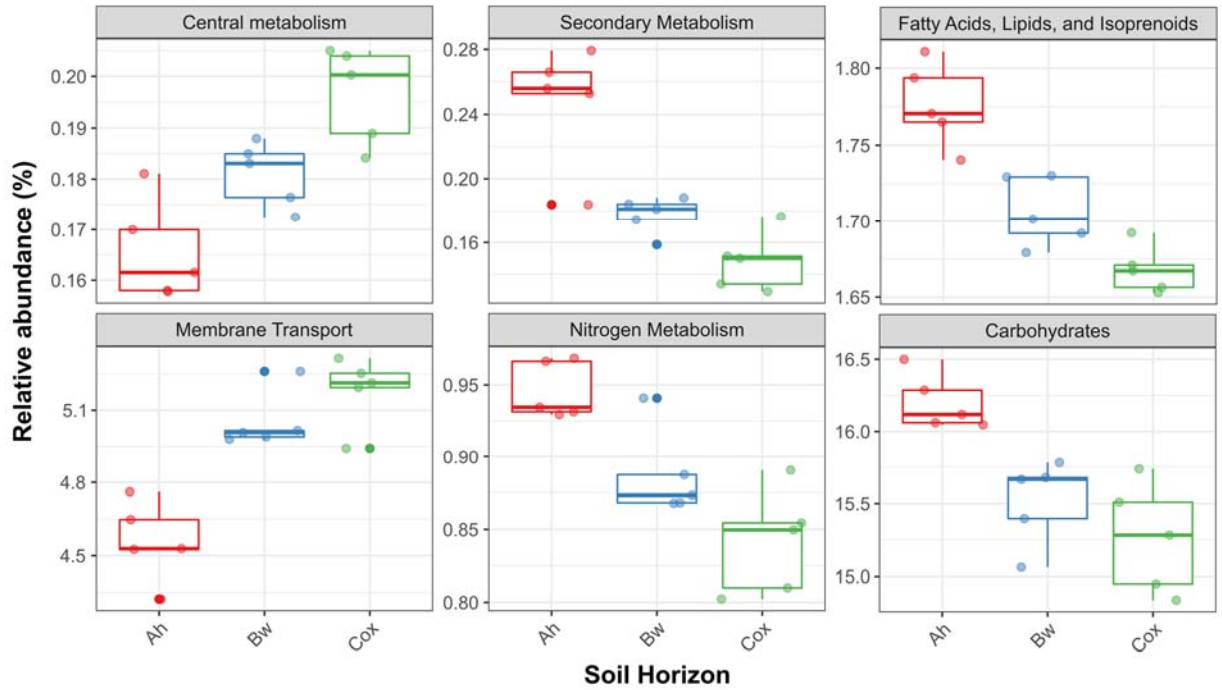

Figure 7: Boxplots of relative abundance of SEED level 1 functional categories. Relative abundance is expressed as a percentage of the total annotated reads. The bottom and top of the boxes represent the first and third quartiles, with the central band representing the median, whiskers represent 1.5 times the interquartile range according to Tukey's boxplot method(Tukey, 1977). All data points are also plotted as jittered points.

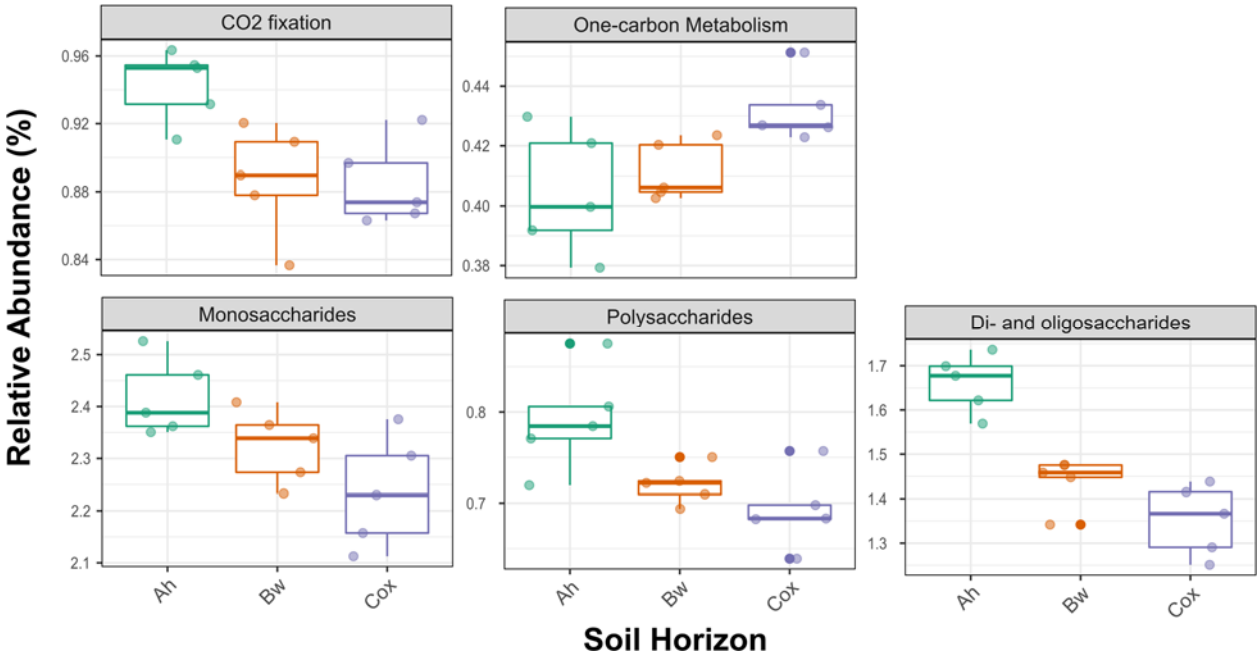

Figure 8: Abundance of SEED level 2 categories related to carbon metabolism. Relative abundance is expressed as a percentage of the total annotated reads. The bottom and top of the boxes represent the first and third quartiles, with the central band representing the median, whiskers represent 1.5 time the interquartile range according to Tukey's boxplot method (Tukey, 1977). All data points are also plotted as points.

787